

## The asymptotic stage of longitudinal turbulent dispersion within a tube

By R. DEWEY AND PAUL J. SULLIVAN

Department of Applied Mathematics, University of Western Ontario, London, Ontario

(Received 31 October 1975 and in revised form 5 November 1976)

This paper describes an experimental investigation of the conditions for which the asymptotic description of longitudinal dispersion given by Taylor (1954) would apply. At non-dimensional times following the release of a dye pulse that are significantly larger than those previously investigated, the integrated concentration curves were observed to be skewed. At relatively short times from release the concentration curves appear to be well described by the models presented by Sullivan (1971) and by Chatwin (1973). Some features of the asymptotic behaviour, namely the translation of the modal value of the integrated concentration curve at the discharge velocity and the constant temporal growth rate of the variance, are observed at the longest times following release. On the basis of these observations it is estimated that a non-dimensional time interval of  $tu_*/d = O(10^5/R_*)$ , where  $R_* = u_*d/\nu$ ,  $u_*$  is the friction velocity,  $\nu$  the kinematic viscosity and  $d$  the tube diameter, is required for the Taylor result to become applicable. Thus application of Taylor's theory is significantly restricted in turbulent flows, especially those with irregular boundaries and those that are not stationary. There the variations in the flow must be small with respect to an equivalent 'development time' if a value of the 'local' longitudinal diffusion coefficient is to have meaning.

---

### 1. Introduction

The asymptotic stage of the longitudinal dispersion of a passive scalar within a bounded turbulent shear flow, such as that in a pipe or channel, is characterized by a Gaussian distribution of the cross-sectionally integrated concentration. The Gaussian distribution is symmetrical about an axis that is translated with the flow discharge velocity and the temporal growth rate of the variance of the distribution is constant. Chatwin (1971) has reviewed measurements of longitudinal dispersion of Fischer (1966) in an open channel and Taylor (1954) in a smooth pipe. He determined that, with the exception of one of Taylor's measurements, these measurements were not characteristic of the asymptotic stage. One would like to find a time scale that is associated with asymptotic behaviour so that one could make an assessment of the conditions under which a 'local' value of longitudinal diffusivity would apply. In such naturally occurring flows as rivers or tidal estuaries one expects that the temporal changes that a marked fluid element would experience, owing to the unsteadiness of the flow or owing to the irregularities of the flow boundaries as it is convected downstream, should be slow with respect to the time interval required for the asymptotic stage to evolve if a 'local' value of diffusivity is to have meaning. One notices, for example, a large

variation of non-dimensional longitudinal diffusivities for rivers and canals listed by Fischer (1973).

A typical marked fluid element is transported over the flow cross-section by the turbulent fluctuating velocities. When the fluid element has traversed the cross-section a number of times, its position on the cross-section becomes independent of the release position. The streamwise displacement  $\xi(t)$  of the fluid element relative to an axis moving with the flow discharge velocity  $\bar{U}$ , and the longitudinal velocity  $U(t) = u(t) - \bar{U}$ , where  $u(t)$  is the instantaneous streamwise component of the velocity of the fluid element, are stationary random variables with zero mean for this fully developed flow (Batchelor, Binnie & Phillips 1955). The autocorrelation function

$$Q(\tau) = \overline{U(t)U(t+\tau)}, \quad (1)$$

where the overbar denotes an ensemble average, becomes zero for  $\tau$  large. Following Taylor (1921, 1954), the longitudinal diffusivity  $D$  is determined from

$$D = \frac{1}{2} \frac{d\overline{\xi(t)^2}}{dt} = \int_0^t Q(\tau) d\tau \quad (2)$$

and is constant for  $t$  large, say  $t > T$ . As a consequence of the central limit theorem, the distribution of marked fluid elements is expected to be Gaussian with a variance equal to  $2Dt$  many time intervals  $T$  after release.

When an initial concentration of a passive scalar, for example a uniform concentration over the plane  $x = 0$ , is dispersed in the turbulent flow, the marked fluid can be considered to be comprised of marked fluid elements. The resulting concentration at a later time can be determined from the superposition of the probable displacements of these marked fluid elements (Batchelor 1949). Thus the integral  $C(x, t)$  of the concentration over the flow cross-section will be a symmetrical Gaussian distribution centred about  $x = \bar{U}t$  and will have a constant value of  $D$  at large downstream distances. Taylor (1954) has solved the diffusion equation, using the Reynolds analogy, to provide an estimate of  $D = 10.1au_*$ , where  $a$  is the radius of a smooth-walled pipe.

At times that are smaller than those required for the asymptotic shape, the  $C(x, t)$  are observed to be skewed towards the release position (Elder 1959; Fischer 1966; Sullivan 1971; Taylor 1954). Chatwin (1971) has demonstrated that some of these measurements are well described by the second stage of a three-stage description of the longitudinal dispersion within a bounded turbulent shear flow given by Sullivan (1971). (See also Chatwin 1973.) The second stage is characterized by a constant velocity

$$v = \frac{2}{(a-\delta)^2} \int_0^{a-\delta} U(r)r dr \quad (3)$$

of  $\bar{C}(x, t)$ , the maximum value of  $C(x, t)$ . Here  $\delta$  is the depth of the viscous layer and  $U(r)$  is the average fluid velocity in a fixed reference frame. The portion of  $C(x, t)$  that is downstream of  $\bar{C}(x, t)$  is of Gaussian form with a constant diffusivity  $D_2 < D$ . The flow cross-section can be considered to be made up of core fluid,  $r < a - \delta$ , and viscous fluid,  $r > a - \delta$ . Marked fluid which is released in the core and remains in this region will sample this area in a time  $O(d/u_*)$ . Marked fluid transported from the core to the viscous region is advected upstream with respect to marked fluid remaining in the core. Thus the forward part of  $C(x, t)$  describes marked fluid contained only in the core region. When a significant amount of marked fluid has passed from the core to the

viscous region, i.e. when the combined effect of the longitudinal dispersion of marked fluid in the core and the efflux of marked fluid from the core has reduced the magnitude of  $\bar{C}(x, t)$  to the extent that it is no longer the prominent feature of  $C(x, t)$ , then a new maximum value of  $C(x, t)$  will develop upstream and represent marked fluid in the core and viscous regions.

An experiment was devised to measure a time interval that would be indicative of the transition from the second stage to the third or asymptotic stage of longitudinal turbulent dispersion. The salient feature that was selected for investigation was the velocity of  $\bar{C}(x, t)$ . This is expected to be constant in both the second and the asymptotic stage. In the experiment the length of pipe and discharge velocities were such that displacements of hundreds of metres and time intervals of minutes were involved in the resolution of experimental data.

## 2. Experimental procedure

A 300 m long conduit, formed from butt-jointed 6.1 m sections of 2.1 cm diameter iron pipe, was suspended horizontally on t-rails and aligned with a theodolite. Flow Reynolds numbers in the range  $15\,000 < R = \bar{U}d/\nu < 37\,000$  were obtained with a jet centrifugal pump.

A neutrally buoyant solution of fluorescein was injected 26.8 m downstream of the flow straightener. This was comprised of a bundle of tubes 0.3 cm in diameter and 10 cm long which were inserted in the iron pipe. The injection device allowed a pressurized pulse of the dye to penetrate well into the core of the pipe flow (see figure 1, plate 1) through six evenly spaced ports on the pipe wall. The device was spring-loaded and generally gave a reproducible result.

Downstream of the injection point a Turner open-door Fluorometer, modified such that the sampling tube of the instrument became a part of the pipe wall, was used to obtain a measure of the dye concentration within the flow. The Fluorometer was tested with known concentrations and produced an electrical signal that was directly proportional to the sample concentrations. When used in the experiment at the tested levels of concentration the Fluorometer produced an electrical signal proportional to the integral over the flow cross-section of the concentration of dye, i.e.

$$C(x, t) = \int_0^a \int_0^{2\pi} C(x, r, \theta, t) r dr d\theta.$$

The electrical signal thus obtained was relayed to a strip-chart recorder and to a digital voltmeter and paper-tape punch.

The release of a dye pulse was communicated by means of a short-range wireless to an operator at the sampling station, and a record of the time interval between dye release and the insertion of a fiducial mark on the record was measured with a stop-watch.

Mean-velocity profiles were measured with an olive-oil manometer and a Pitot tube which was positioned on the flow cross-section with a micrometer head. For higher flow rates a 'bellows' type manometer was used to obtain this profile. The discharge velocity was measured by recording the amount of time taken to fill a barrel of known volume. Total pressure was recorded at all of the sampling stations and the total inlet pressure was monitored regularly to ensure that steady flow conditions prevailed. These

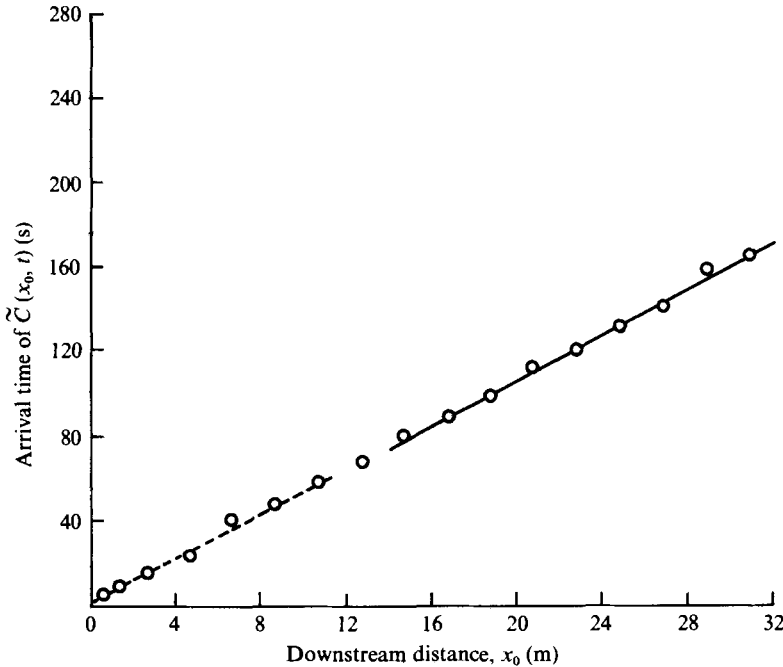


FIGURE 2. The arrival time of the maximum value of the integrated concentration.  $R_* = 724$ . ---, second-stage velocity of 189.36 cm/s; —, discharge velocity of 183 cm/s.

measurements were typical of a fully developed turbulent flow through a smooth-walled pipe. An elaboration of the experimental details is given in Dewey (1975).

### 3. Experimental results

Dyed fluid was injected into the pipe and the integrated concentration curves  $C(x_0, t)$  were recorded at fixed distances  $x_0$  downstream. Graphs of displacement against arrival times of the maximum value of  $C(x_0, t)$ , i.e.  $\tilde{C}(x_0, t)$ , indicated the presence of both the second and the third stage of longitudinal dispersion (see figure 2). In table 1 a comparison is made between the velocities of  $\tilde{C}(x_0, t)$  determined from the displacement-time records and the measured flow discharge velocity as well as the value of  $v$  calculated from (3) with

$$\delta = 15\nu/u_* \quad \text{and} \quad U(r)/u_* = 2.5 \ln [(a-r)u_*/\nu] + 5.5.$$

The value of the velocity of the centre of mass of  $C(x_0, t)$  was also measured and is included in table 1 for comparison with the discharge velocity.

The experimental accuracy in measuring velocities from the concentration records is approximately  $\pm 1\%$ . The most significant source of error occurred when changing sampling stations. This procedure involved interchanging the section of pipe containing the sampling equipment with the pipe section at the next sampling station. The major error resulted from the inexact reproduction of identical flow conditions. This error is evidenced in the experimental scatter observed in figures 2 and 5(c).

$R_*$	415	420	724	804 (T2)	820	967	1204 (T1)
$v^{(1)}$	103	103	189	—	218	261	—
$v^{(2)}$	104	106	190	—	216	N.A.	—
$u^{(1)}$	97.5	98.4	183.8	136	211.5	254.8	222
$u^{(2)}$	N.A.	100	183	—	207	250	—
$u^{(3)}$	—	—	180	137.8	210	250	221
$u_*$	5.81	5.84	10.07	8.45	11.42	13.45	12.65

$v^{(1)}$  Value calculated using (3) and  $\delta = 15\nu/u_*$ .

$v^{(2)}$  Measured value.

$u^{(1)}$  Measured value of discharge velocity found using barrel of known volume.

$u^{(2)}$  Value of discharge velocity estimated from the velocity of the centre of mass of the dispersing dye pulse.

$u^{(3)}$  Value of discharge velocity estimated from the displacement-time records at the furthest most downstream stations.

T1 Values from Taylor (1954) as given by Chatwin (1971) in his figure 4.

T2 Values from Taylor (1954) as given by Chatwin (1971) in his figure 3.

N.A. Entry not available.

Note: all velocities are given in cm/s.

TABLE 1

A transition time  $t_*$  was determined from the displacement-time records of  $\tilde{C}(x_0, t)$ . Typically these records (see figure 2) contain an initially linear segment followed by a transition or nonlinear segment, ending in another linear segment. For  $n$  data points  $(x_{0i}, t_i)$  of which the first  $n_1$  are nearly linear,  $n_1$  to  $n_2$  are nonlinear and  $n_2$  to  $n$  are linear, a least-squares fit of the subset of data points at each end of the record to a straight line is expected to have small residuals. A least-squares fit to the first  $K$  data points is given by

$$t = a + bx_0, \quad (4)$$

where  $a$  and  $b$  are determined by the solution of

$$\sum_{i=1}^K t_i = Ka + b \sum_{i=1}^K x_{0i}, \quad (5)$$

and

$$\sum_{i=1}^K x_{0i} t_i = a \sum_{i=1}^K x_{0i} + b \sum_{i=1}^K x_{0i}^2. \quad (6)$$

The average residual is given as

$$S_K = \frac{1}{K} \sum_{i=1}^K (t - t_i)^2. \quad (7)$$

When  $K > n_1$  the value of  $S_K$  is expected to increase. When the same procedure is used to fit  $t = c + dx_0$  starting with the  $n$ th data point and progressively including those data points with smaller index  $i$  the residuals become

$$S_P = \frac{1}{n-P} \sum_{i=P}^n (t - t_i)^2. \quad (8)$$

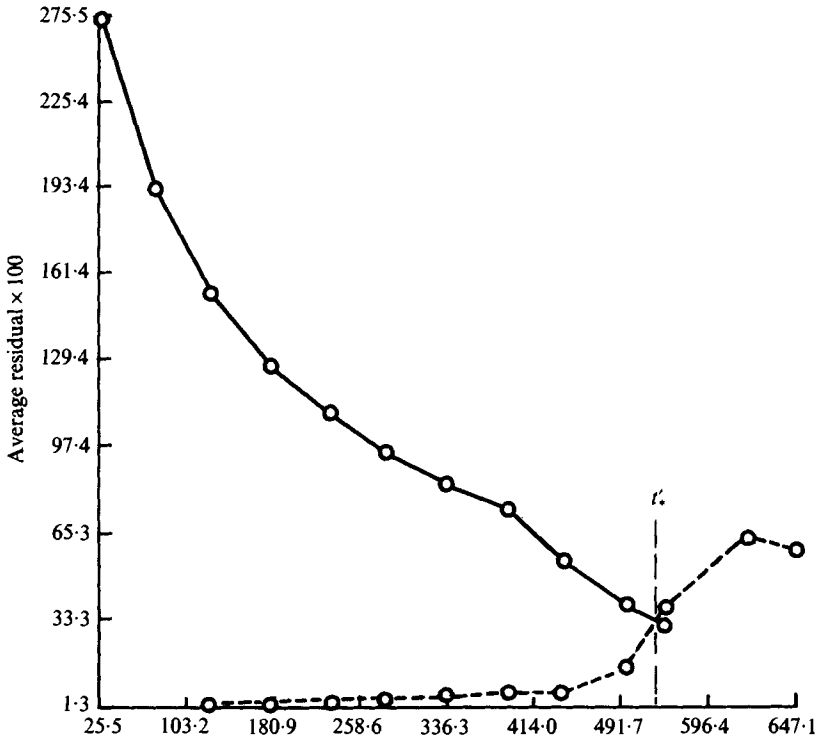


FIGURE 3. The residuals when a least-squares fit is made to arrival time against displacement data from a forward and backward direction.  $R_* = 820$ .  $t' = tu_*/d$ .

When  $P < n_2$  the value of  $S_P$  is expected to increase. The value of  $t$  at which  $S_K = S_P$  determines an elapsed time  $t_*$  that is between the second and third stage. Figure 3 shows a typical sequence of  $S_P$  and  $S_K$  values; the point of intersection determines the value of  $t_*$ .

The asymptotic stage of longitudinal dispersion is expected to occur after an interval of time sufficiently large for a typical marked fluid element to have sampled the entire flow cross-section including the viscous region. This time interval can be represented as  $t_* = t_c + t_v$ , where  $t_c$  is the time required to sample core fluid and  $t_v$  the time required to sample the fluid contained in the viscous layer.  $t_c$  is  $O(d/u_*)$  and is considered negligible with respect to  $t_v$ , which is  $O(\delta^2/\kappa)$ , where  $\kappa$  is the coefficient of mass diffusivity. Thus

$$t_* = O\left(\frac{\delta^2}{\kappa}\right) = O\left(\left(\frac{15d}{R_*}\right)^2 \frac{1}{\kappa}\right)$$

and

$$t'_* = \frac{t_* u_*}{d} = O\left(\frac{225 \nu}{R_* \kappa}\right).$$

Assuming the Schmidt number  $\nu/\kappa$  to be  $O(10^3)$  for liquids gives

$$t'_* = O(10^5/R_*). \tag{9}$$

The measured values of  $t'_*$  plotted in figure 4 are all of order  $10^5/R_*$ . The straight line in figure 4 has a slope of approximately  $1.4 \times 10^6$  (and so has an equation of the form

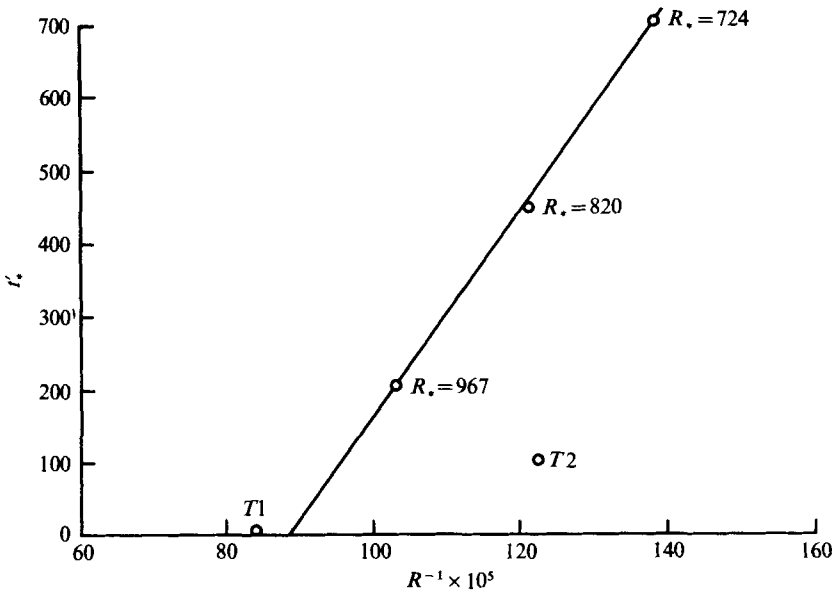


FIGURE 4. A non-dimensional time scale  $t'_*$  derived from the intersection of curves of the type shown in figure 3.  $T1$  and  $T2$  refer to Taylor's values; see table 1.

$t'_* = t'_{*0} + 1.4 \times 10^6/R_*$ , which is consistent with the order-of-magnitude argument leading to (9), bearing in mind the limited number of measured points over a relatively narrow range of  $R_*$ .

The velocities of  $\bar{C}(x, t)$  that were measured at  $R_* = 415$  and  $R_* = 420$  were found to be approximately equal to those calculated from (3) throughout the entire length of pipe. Figure 4 indicates that a time interval which was not experimentally attainable ( $t'_* \sim 2000$ ) would be required for the transition at these values of  $R_*$ .

The definition and measurement of a transition time scale  $t_*$  was based on the velocity of  $\bar{C}(x_0, t)$  because this is experimentally the most accessible feature of  $C(x, t)$ . When  $C(x, t)$  is in the final asymptotic stage it is expected to be a symmetrical Gaussian curve and the longitudinal diffusivity is expected to be constant. However, the experimental curves of  $C(x_0, t)$  were not found to be completely symmetrical even at the most distant locations downstream, so that it takes a longer time than  $t_*$  for complete symmetry to be established. The shape of  $C(x, t)$  is evolving in both space and time such that recording the concentration at a fixed point as a function of time could misrepresent  $C(x, t)$ . That is, the longitudinal dispersion that takes place during the recording time could give rise to a significant distortion of the recorded  $C(x_0, t)$ , particularly at the sampling stations furthest downstream.

The asymptotic form is

$$C(x, t) = At^{-\frac{1}{2}} \exp\{-(x - \bar{U}t)^2/4Dt\}, \tag{10}$$

where  $A$  is a constant determined from the total amount of passive-scalar marker. Considering the measurement to be made at a fixed downstream distance  $x_0$ , (10) becomes

$$C(x_0, t) = At^{-\frac{1}{2}} \exp\{-(x_0 - \bar{U}t)^2/4Dt\}. \tag{11}$$

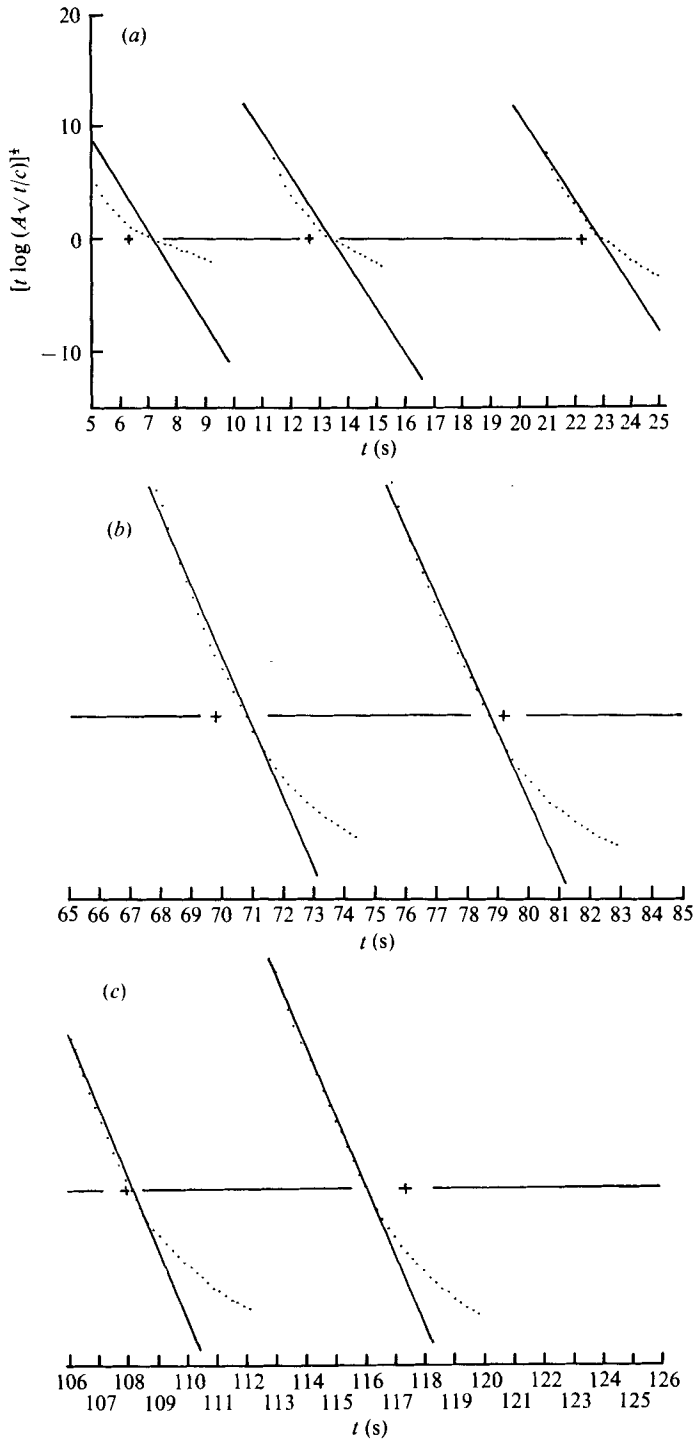


FIGURE 5. A series of station samples presented as the variable suggested by Chatwin (see §3).  $R_* = 820$ .



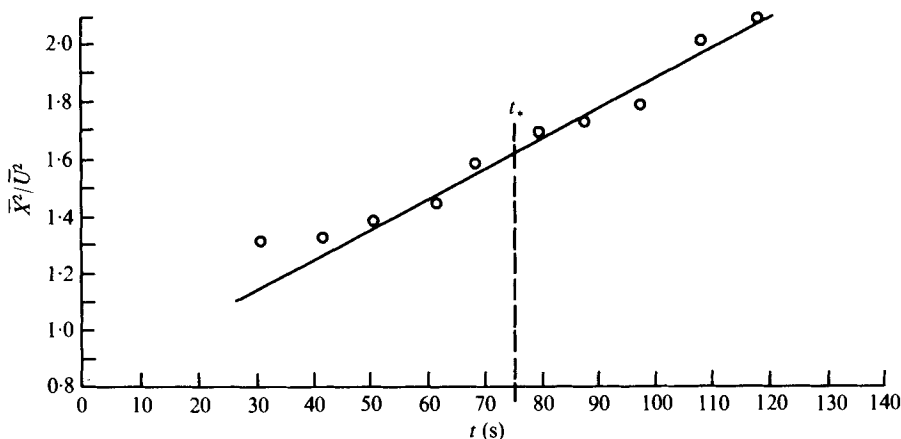


FIGURE 6. The growth of the variance of the part of  $C(x_0, t)$  downstream of  $\tilde{C}(x_0, t)$  measured from the position of  $\tilde{C}(x_0, t)$ .  $R_* = 820$ .

Following Chatwin (1971), (11) can be written in the form

$$\left[ t \ln \left( \frac{At^{-\frac{1}{2}}}{C(x_0, t)} \right) \right]^{\frac{1}{2}} = \frac{x_0}{2D^{\frac{1}{2}}} - \frac{\bar{U}t}{2D^{\frac{1}{2}}}, \quad (12)$$

such that a graph of the left-hand side of (12) against  $t$  will be linear with a slope of  $-\bar{U}/2D^{\frac{1}{2}}$  and will cross the time axis at  $t = x_0/\bar{U}$ . This procedure, as given by Chatwin (1971), eliminates the assumption usually made in taking fixed-point measurements of turbulent dispersion that the longitudinal dispersion that occurs during the recording interval is negligible. The results taken at 7 experimental stations for one flow Reynolds number are shown on figure 5. A plus sign on the time axis indicates the calculated value of  $x_0/\bar{U}$ , where  $\bar{U}$  is the measured discharge velocity. The solid line on each record has a slope of  $-\bar{U}/2D^{\frac{1}{2}}$ , where  $D$  was measured from the rate of change of the second moment of the downstream part of  $C(x_0, t)$  about the position of  $\tilde{C}(x_0, t)$ . That is,  $D$  is the longitudinal diffusivity estimated from data at  $t > t_*$ . As the time following release is increased in figure 5 the data points appear to be more completely described by the solid line. The departure of the data points from the solid line, corresponding to an upstream skewness in  $C(x, t)$ , is present even at the furthestmost sampling stations. Thus at no time were completely Gaussian curves for  $C(x, t)$  observed. The growth rate of the variance when the forward, and thus non-skewed, part of  $C(x_0, t)$  was used does appear to be constant for  $t > t_*$ , as the typical sample record in figure 6 shows.

One advantage of the measuring technique that was used here is that it provides a direct measure of the integral of the concentration. In the measurements of both Fisher (1966) and Taylor (1954) a fixed probe that recorded the concentration at one point on the flow cross-section was used. The assumption that the marked fluid is uniformly mixed over the flow cross-section is required for the interpretation of single-point measurements. The difference in measuring technique could explain why the measurements made at the pipe centre-line by Taylor (1954) appear to be less skewed, at comparatively shorter distances downstream, than those presented herein.

When applied to the asymptotic stage, the expression for  $D$  given in the introduction becomes

$$D = \int_0^\infty \overline{U(t)U(t+\tau)} d\tau = \overline{U}^2 \int_0^\infty \left( \frac{\overline{U(t)U(t+\tau)}}{\overline{U}} \right) d\tau = \overline{U}^2 \overline{T}, \quad (13)$$

where  $\overline{T}$  is a time.

Now when the viscous layer is neglected  $\overline{T}$  must be  $O(d/u_*)$ . Thus

$$D = O((\overline{U}d)^2/u_*d),$$

or

$$D' = D/u_*d = O((\overline{U}/u_*)^2). \quad (14)$$

Consider, on the other hand, the unrealistic case where the value of  $\overline{T}$ , defined in (13), is essentially dominated by the effects of the viscous layer. Then taking  $t_*$  as an estimate for  $\overline{T}$  gives

$$D = O(\overline{U}^2d/u_*R_*),$$

or

$$D' = O(\overline{U}/u_*^2R_*). \quad (15)$$

In practice calculations by Chatwin (1971) suggest that the viscous sublayer makes a contribution of 10–20% to  $D$ , so that it can be anticipated that the scaling in (14) will normally be the appropriate one, although the shape of the graph of  $D/u_*d$  against  $(\overline{U}/u_*)^2$  can be expected to depend slightly on the values of  $R_*$  and  $\nu/\kappa$  because there will be some dependence on the viscous sublayer, and the magnitude of this dependence will change with  $R_*$ .

#### 4. Discussion

It is interesting to notice that if the dispersion takes place in a hypothetical flow with no molecular diffusion and with complete Reynolds number similarity (Townsend 1956, p. 196), then the value  $(\overline{U}/u_*)^2$  is independent of  $R_*$  and the result of Taylor (1954) that  $D'$  is a constant, i.e. that  $D = O(u_*d)$ , is obtained from (14). This result is also clear in these circumstances on dimensional grounds. In a rough-walled tube, therefore, the value of  $D'$  is independent of  $R_*$ , but it does depend in principle on the ratio  $h/d$ , where  $h$  is the roughness height. (However the available experimental evidence suggests that this dependence is very weak.)

For a flow in which complete Reynolds number similarity does not hold (but still with no molecular diffusion)  $(\overline{U}/u_*)^2$  varies with the flow conditions, so that in a smooth-walled tube  $(\overline{U}/u_*)^2 = f(R_*)$ , and (14) shows that  $D'$  then depends on  $R_*$ .

Equation (13) applies equally well to the dispersion of a passive contaminant in a laminar flow. There  $\overline{T} = O(d^2/\kappa)$  and  $D_L = O(\overline{U}^2d^2/\kappa)$ , which is the result found by Taylor (1953). Taylor clearly pointed out that longitudinal dispersion is governed by the interaction of the gradients in mean velocity with the cross-stream diffusion. In the case of laminar flow one can consider  $D_L$  to be given by the ratio of the square of a term representing the dispersion by the mean shear ( $Ud$ ) to a term representing the lateral diffusion ( $\kappa$ ). By comparison the expression (14) for  $D$  is the ratio of the square of  $\overline{U}d$  to a term representing the lateral diffusion due to turbulent velocities ( $u_*d$ ).

All the experimental values of  $D'$  determined with  $t' > t'_*$  in the manner described after (12) except that for  $R_* = 420$  are shown on figure 7 and appear to increase with increasing values of  $(\overline{U}/u_*)^2$  (see Sullivan 1971). The value of  $D'$  for  $R_* = 420$  is clearly

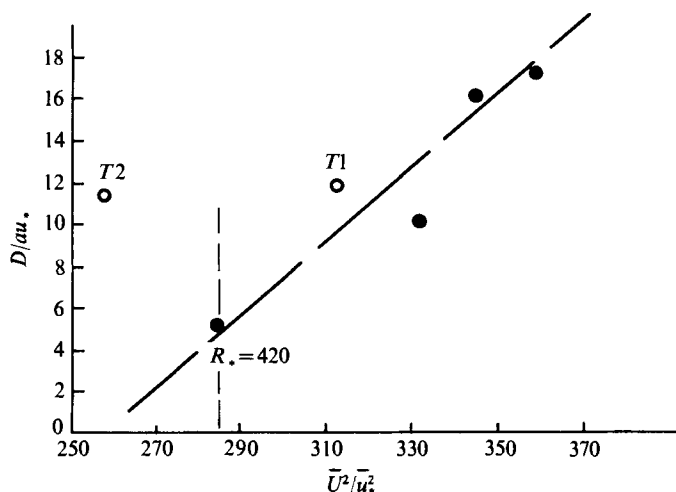


FIGURE 7. Comparison of (14) with the authors' experimental results. ●, values of  $2D/du_*$ . The points labelled T1 and T2 are taken from experiments by Taylor (1954).

a second-stage value. These relatively few values are not considered to be reliable enough to test critically the validity of (14). One can only conclude that the measured results are not inconsistent with (14), and these are believed to be the most comprehensive measurements available.

The measured values of  $t'_*$  are indicative of transition to an asymptotic state of turbulent dispersion as measured by the velocity of  $\bar{C}(x, t)$ . In a review of Taylor's data Chatwin (1973) suggested that the transition to the asymptotic stage, as measured by the symmetry of  $C(x, t)$ , appeared to take place at  $t' = 100$ . In these experiments at approximately twice the Reynolds number available to Taylor it is found that a non-dimensional time that is a factor of at least three larger is required for symmetry to be observed. This large time is closely related to the size of the viscous layer.

This work received financial support from the National Research Council of Canada. The authors are indebted to Dr P. C. Chatwin for his helpful discussion of the work.

#### REFERENCES

- BATCHELOR, G. K. 1949 *Austr. J. Sci. Res.* **2**, 437.  
 BATCHELOR, G. K., BINNIE, A. M. & PHILLIPS, O. M. 1955 *Proc. Phys. Soc.* **B68**, 1095.  
 CHATWIN, P. C. 1971 *J. Fluid Mech.* **48**, 689.  
 CHATWIN, P. C. 1972 *J. Fluid Mech.* **51**, 63.  
 CHATWIN, P. C. 1973 *Quart. J. Mech. Appl. Math.* **26**, 427.  
 DEWEY, R. 1975 M.Sc. thesis, University of Western Ontario.  
 ELDER, J. W. 1959 *J. Fluid Mech.* **5**, 544.  
 FISCHER, H. B. 1966 *Caltech Rep.* KH-R-12.  
 FISCHER, H. B. 1973 *Ann. Rev. Fluid Mech.* **5**, 59.  
 SULLIVAN, P. J. 1971 *J. Fluid Mech.* **49**, 551.  
 TAYLOR, G. I. 1921 *Proc. Lond. Math. Soc.* Ser. 2, 196.  
 TAYLOR, G. I. 1953 *Proc. Roy. Soc.* **A219**, 186.  
 TAYLOR, G. I. 1954 *Proc. Roy. Soc.* **A223**, 446.  
 TOWNSEND, A. A. 1956 *The Structure of Turbulent Shear Flow*. Cambridge University Press.



FIGURE 1. A view through a transparent section of the pipe showing the dye pulse at less than 1 m from the injection device.